SF2A 2008
C. Charbonnel, F. Combes and R. Samadi (eds)

WAVEFRONT RECONSTRUCTION WITH ELONGATED SODIUM LASER GUIDE STARS

Tallon, M.[1], Tallon-Bosc, I.[1], Béchet, C.[1] and Thiébaut, E.[1]

Abstract. When forming a sodium laser guide star (LGS), the lightened volume in this layer can be seen as a cylindrical source ∼1m in diameter and ∼10 km in length. Because of the parallax, the LGS looks significantly elongated when observed from the edge of the pupil of an Extremely Large Telescope. This effect prompts the lasers to be launched from behind the secondary instead of from around the telescope, but still degrades significantly the accuracy of wavefront sensing for adaptive optics. Further, the measurement uncertainties are no more uniform across the pupil and correlations are introduced. From numerical simulations, we analyze the benefit of taking into account these structured correlations and the effect of priors in wavefront reconstruction algorithms. We found that priors are effective for a single LGS launched behind the secondary. When combining the measurements from several LGSs in a Ground Layer adaptive optics system, we found that taking into account the noise covariances and launching from the edge yields the best reconstruction. Further, in this configuration, we can discard the worse measurements along the elongated direction and reduce the field of view (thus use a smaller detector) without any significant loss of accuracy.

1 Introduction

Extremely Large Telescopes (ELT) all rely on adaptive optics systems using several laser guide stars (LGS). But since the atmospheric sodium atoms are concentrated at ∼90 km in altitude, in a ∼ 10km thick layer (Papen et al. 1996), a LGS is seen as a significantly elongated spot from the edge of an ELT (Fig. 1).

The elongation of the spots at the focus of the subapertures of a Shack-Hartmann wavefront sensor significantly reduces the accuracy on the measurement of the centroid displacements. Furthermore, much larger detectors are necessary to image the enlarged spots. New centroiding algorithms like the matched filter (Gilles & Ellerbroek 2006) have been devised to cope with the increase of reading noise, but the magnitude of photon noise – proportional to the size of the spots (Rousset 1999) – is much higher.

Our aim is here to assess the effect of the spot elongation on the reconstructed wavefront. Since the elongations vary in amplitude and orientation (Fig. 1), the noise is no more uniform across the pupil and correlations appear between x and y coordinates of the measured gradients of the wavefront. We show that introducing Kolmogorov (or von Kármán) priors and taking into account the actual noise correlations dramatically improve the quality of the reconstruction, compared to ignoring them. From numerical simulations, we compare the wavefront reconstruction capability of different methods and show that unexpected better results can be obtained when the LGSs are launched from the edge of the telescope pupil, although all the current ELT projects expect to minimize the problem by launching the LGS from the center, behind the secondary. Furthermore, we show that truncating the spots with smaller detectors does not degrade significantly the results.

2 Reconstruction methods and assumptions

In the following, we will compare four reconstruction methods, introducing priors or not, and taking into account actual noise correlations or not. All of them start with the same model of data:

$$\boldsymbol{d} = \mathbf{S} \cdot \boldsymbol{w} + \boldsymbol{n}, \tag{2.1}$$

[1] Université de Lyon, Lyon, F-69003, France ; Université Lyon 1, Observatoire de Lyon, 9 avenue Charles André, Saint-Genis Laval, F-69230, France ; CNRS, UMR 5574, Centre de Recherche Astrophysique de Lyon ; Ecole Normale Supérieure de Lyon, Lyon, F-69007, France

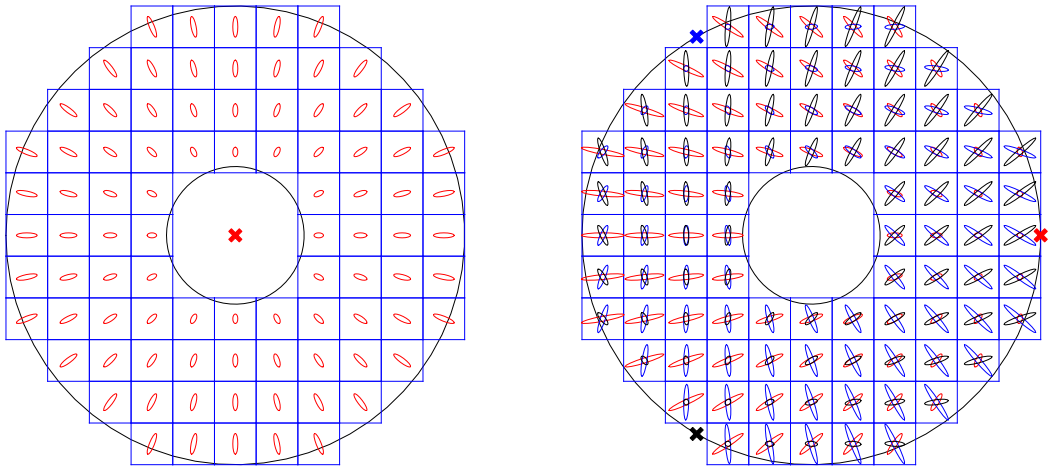

Fig. 1. Layout of the elongated spots for centered LGSs (left) and for three LGSs launched at 120° from the edge of the pupil (right). The diameter of the pupil is 42m with 30% central obstruction. In the two cases, $h_0 = 90$ km, the FWHM of the Sodium layer is 10 km, and the minimal FWHM of the spots is 1.2″ (spot size with no elongation). This configuration with 11×11 subapertures is chosen to be illustrative, but 100×100 subapertures are used for the simulations. Here, the field of view of the 3.8m subapertures is 10″, and the squares represent both the subapertures and their field-of-view limits. Launching from the center minimizes the elongation and produces radially elongated spots: this is the chosen configuration for the Thirty Meter Telescope (TMT) (Gilles & Ellerbroek 2006).

where the vector of data, $\boldsymbol{d}$, is obtained from the vector of wavefront samples on a suitable grid, $\boldsymbol{w}$, using a linear model $\mathbf{S}$ of the wavefront sensor. Vector $\boldsymbol{n}$ stands for an additive zero-mean noise independent from the data. We will assume a Shack-Hartmann wavefront sensor with Fried's geometry for $\mathbf{S}$ (Fried 1977).

We consider four different methods to invert Eq. (2.1), corresponding to the following equations:

$$\left(\mathbf{S}^{\mathrm{T}} \cdot \mathbf{S}\right) \cdot \boldsymbol{w} = \mathbf{S}^{\mathrm{T}} \cdot \boldsymbol{d}, \qquad \text{for pure least squares,} \tag{2.2}$$

$$\left(\mathbf{S}^{\mathrm{T}} \cdot \mathbf{C}_{\boldsymbol{n}}^{-1} \cdot \mathbf{S}\right) \cdot \boldsymbol{w} = \mathbf{S}^{\mathrm{T}} \cdot \mathbf{C}_{\boldsymbol{n}}^{-1} \cdot \boldsymbol{d}, \qquad \text{for weighted least squares,} \tag{2.3}$$

$$\left(\mathbf{S}^{\mathrm{T}} \cdot \mathbf{C}_{\boldsymbol{n}}^{-1} \cdot \mathbf{S} + \mathbf{C}_{\boldsymbol{w}}^{-1}\right) \cdot \boldsymbol{w} = \mathbf{S}^{\mathrm{T}} \cdot \mathbf{C}_{\boldsymbol{n}}^{-1} \cdot \boldsymbol{d}, \qquad \text{for maximum } \textit{a priori} \text{ (MAP),} \tag{2.4}$$

$$\left(\mathbf{S}^{\mathrm{T}} \cdot \mathbf{S} + \sigma_n^2 \mathbf{C}_{\boldsymbol{w}}^{-1}\right) \cdot \boldsymbol{w} = \mathbf{S}^{\mathrm{T}} \cdot \boldsymbol{d}, \qquad \text{for MAP with uniform noise.} \tag{2.5}$$

Equations (2.2) and (2.5) assume uniform Gaussian noise. The equations are written in the form $\mathbf{A} \cdot \boldsymbol{x} = \boldsymbol{y}$ where we are looking for $\boldsymbol{x}$. Indeed, we solve them with the conjugate gradient method (Barrett et al. 1994). This yields the "minimum norm" solution (*i.e.* the method is equivalent to use the pseudo-inverse of $\mathbf{A}$) when $\mathbf{A}$ is not invertible. Also, the conjugate gradient method does not need to compute the inverse of $\mathbf{A}$ which is a huge matrix in our ELT case ($\sim 2\ 10^4 \times 10^4$ for our 100×100 subapertures wavefront sensor). For computing efficiency, we use the Fractal Iterative Method (Tallon et al. 2007), a preconditioned conjugate gradient method using a so-called fractal operator and an optimal diagonal preconditioner.

In our simulations, we introduce some simplifications to only focus on the effect of the spot elongations. We assume that the LGSs can measure tip/tilts and that all the turbulence is in the pupil plane. Thus the results are not affected by any focus anisoplanatism or tip/tilt indetermination. We also assume a Gaussian distribution of the vertical density profile of the sodium atoms, centered at altitude 90 km, and spots with elongated Gaussian shapes at the focus of the 100×100 subapertures of the Shack-Hartmann wavefront sensor. The actual noise covariance matrix $\mathbf{C}_{\boldsymbol{n}}$ is determined by assuming that the noise is proportional to the size of the spot (Rousset 1999). Seeing is set to 0.7″ at 589 nm (i.e. $r_0 = 17.4$ cm at 589 nm), corresponding approximately to median conditions at Paranal observatory, with an outer scale $L_0 = 22$m.

3 Simulation results

From the same simulated data, the aim is to compare the errors of the wavefront reconstructions obtained with the different reconstruction algorithms listed in Sec. 2.

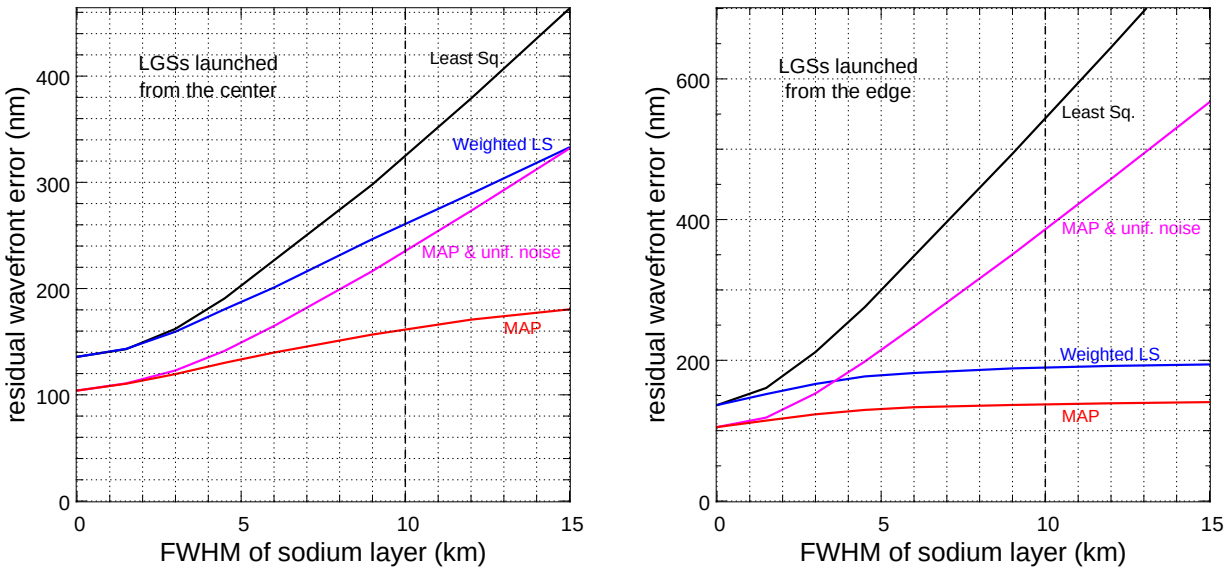

Fig. 2. Comparison of the wavefront errors obtained with the different reconstruction methods, depending on the amount of elongation. On the left, one LGS launched from the center. The same curves are obtained when combining three LGSs three times fainter (noise variance three times higher). On the right, three LGSs launched from the edge. Corresponding configurations are shown on Fig. 1. Noise covariance matrix is only used for *Weighted LS* (Eq. 2.3) and *MAP* (Eq. 2.4), while priors are only used for *MAP* and *MAP+uniform noise* (Eq. 2.5). The dashed vertical line corresponds to the typical mean FWHM of sodium density profile.

Results for a single LGS launched from the center of the pupil are shown in Fig. 2 (left) as a function of the amount of elongation (FWHM of the sodium layer is varied from 0 to 15 km). Noise has been fixed to 1 rad^2/subaperture where no elongation, with a spot size of 1.2″ FWHM. This phase error at 589 nm corresponds to $\sim 0.046''$rms of jitter, or ∼94 nm rms of wavefront error, measured as the rms path difference between the edges of the subapertures. The signal to noise ratio per subaperture is ~ 5.5.

If we consider the FWHM for the mean sodium profile (10 km), we can see a significant difference between the worse method (*Least Squares*) where the elongation increases the wavefront error by a factor of 2.4, and the best method (*MAP*) where this factor is only 1.6. For such an elongation, *MAP* gives a wavefront error half as big as *Least Squares*. When no elongation, we can see that using priors (MAP methods) allows the variance of the error to be reduced by almost a factor of two as already found by Béchet et al. (2007). The curves show that the usefulness of the priors increases with the elongation. We interpret this behavior by an increasing error on the radial modes because of the radial elongation: priors allow reducing this error by using covariances with the other modes that are less affected by the elongation.

If we equally split the light of this single LGS into 3 LGSs launched from the center, the variance of the noise will be three times higher, *i.e.* 3 rad^2/subaperture at 589 nm. Since the three LGSs will give three times the same radially elongated spots (Fig. 1, left), the combination of the three independent measurements will give again the same results (Fig. 2, left). We expect that launching these fainter LGSs from the edge (Fig. 1, right) will improve the reconstruction since each subaperture will see three spots elongated in different directions. This is shown on Fig. 2 (right). The use of the noise covariances is now critical. Indeed, not to take into account the noise covariances makes the residual wavefront errors to be much higher (*Least Squares* and *MAP with uniform noise* methods). The noise covariance matrix allows the reconstruction to properly weight the measurements in each subaperture in order to take into account mainly the measurements in the most accurate directions (*i.e.* the directions perpendicular to the elongations). We can notice that *MAP* method with any elongation gives a better reconstruction than using least squares (weighted or not) without elongation.

Further, when the actual noise covariances are used, Fig. 2 shows an asymptotic behavior as the sodium profile FWHM increases, indicating that as soon as the elongation is significant, the relative weight of the corresponding measurement is so small that it has no more influence. Yet increasing the elongation does no more degrade the situation. In such a regime, we could then set to zero the weights on these measurements

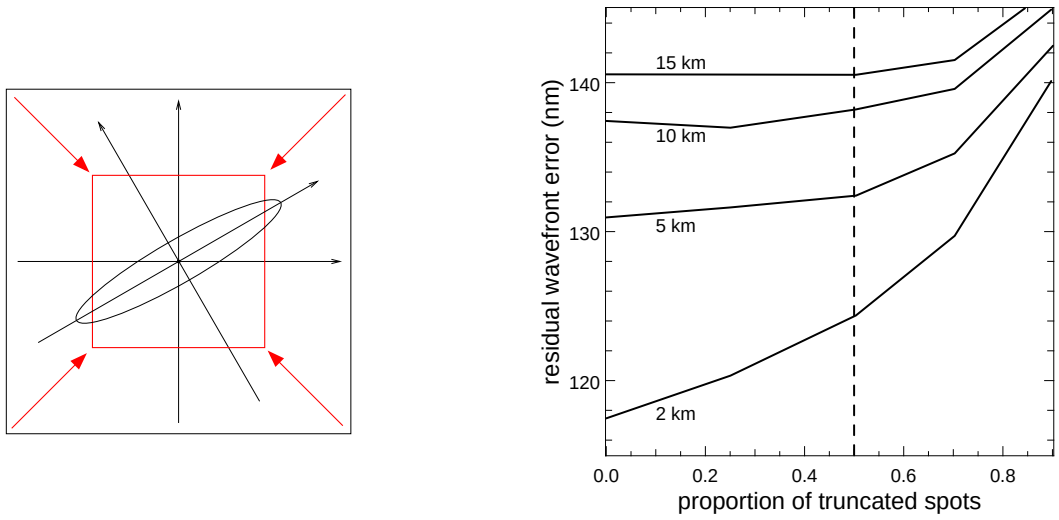

Fig. 3. Reducing the field-of-view truncates the most elongated spots (left) and prevent the measurement of its displacement along the elongation. Simulations (right) show that the quality of the reconstruction is not significantly degraded if 50% of the spots are truncated. The increase for higher proportions is due to the loss of photons.

without significant loss of accuracy. This also means that we should not even need these measurements, so that we could reduce the size of the detectors even if the spots are truncated (Fig. 3, left). We consider in this simulation that a spot is truncated if it is cut at more than 1% of its maximum. Figure 3 shows that the quality of the reconstruction is not significantly degraded if 50% of the spots are truncated.

4 Conclusion

This work shows that, even if priors are helpful, using the actual noise covariances in the reconstruction algorithm is critical. When combining several LGSs launched from the edge of the pupil, the effect of the elongation is then mitigated, even if we use detectors as small as those used when launching from the center, so truncating 50% of the spots.

This activity is supported by the European Community (Framework Program 6, ELT Design Study, contract No 011863). The algorithms and the simulations presented in this article have been implemented in Yorick, a free data processing language written by D. Munro (http://sourceforge.net/projects/yorick/).

References

Barrett, R., Berry, M., Chan, T. F., et al. 1994, Templates for the Solution of Linear Systems: Building Blocks for Iterative Methods (SIAM, Philadelphia PA)

Béchet, C., Tallon, M., & Thiébaut, E. 2007, in Signal Recovery and Synthesis, ed. B. L. Ellerbroek & J. C. Christou, OSA topical meetings (Optical Society of America, Washington, USA), paper JTuA4

Fried, D. L. 1977, J. Opt. Soc. Am., 67, 370

Gilles, L. & Ellerbroek, B. 2006, Appl. Opt., 45, 6568

Papen, G. C., Gardner, C. S., & Yu, J. 1996, in Adaptive optics, O.S.A. topical meeting (Optical Society of America, Washington, USA), 96–99

Rousset, G. 1999, in Adaptive Optics in Astronomy, ed. F. Roddier (Cambridge University Press), 91–130

Tallon, M., Thiébaut, E., & Béchet, C. 2007, in Adaptive Optics: Analysis and Methods, ed. B. L. Ellerbroek & J. C. Christou, OSA topical meetings (Optical Society of America, Washington, USA), paper PMA2